SI Methods

Purification and crystallization of the bimagrumab Fab. The light- (residues 1 to 216, C216A variant) and heavy-chain (residues 1 to 219, R212K variant) of the Bimagrumab Fab were cloned on a polycistronic, periplasmic expression vector with a carboxy-terminal FLAG-tag followed by a His6-tag and expressed in E. coli TG1-. Cells were cultivated at 25°C in SB medium with chloramphenicol and expression was induced with 0.5mM IPTG. Cell pellets were suspended in 150ml lysis buffer (20mM NaH2PO4, 10mM imidazole, 500mM NaCl, pH 7.4, with benzonase and 1 tablet of EDTA-free complete protease inhibitor cocktail (Roche) per 50ml buffer), and disrupted by sonication on ice. After centrifugation at 4°C, the supernatant was sterile filtered and loaded on a 2ml HisTrap column (GE-Healthcare) equilibrated with lysis buffer. After a washing step with 20mM imidazole, the Fab was eluted with a 20 to 500mM imidazole gradient. Fractions were analyzed by SDS-PAGE (NuPage, Invitrogen), pooled, concentrated by ultrafiltration, and further purified over a MonoS cation exchange chromatography column equilibrated with 50mM MES pH 6.0. The Fab was eluted by a 0-1.0M NaCl gradient. For crystallization screening, the buffer was changed to 10mM Tris pH 7.4, 25mM NaCl and the Fab was concentrated to 9.8mg/ml by ultrafiltration. Crystals were grown in 96-well plates (Innovadyne SD2 plates) by sitting drop vapor diffusion. In detail, 0.2µl of protein was mixed with 0.2µl of reservoir solution, and the drop was equilibrated against 80µl of the same reservoir solution at 20°C. The experiments were set up with a Phoenix robotic system (Art Robbins Instruments), stored in a RockImager hotel (Formulatrix) and imaged automatically. Orthorhombic Fab crystals grew from 18% PEG 5,000 monomethylether (MME), 50mM Tris pH 8.0. For X-ray data collection, one

crystal was briefly transferred to a 1:1 mix of the reservoir solution with 20% PEG 5,000 MME, 40% glycerol, mounted in a cryo-loop and flash cooled into liquid nitrogen.

Expression and Purification of the ActRIIA-LBD. The ActRIIA-LBD (Uniprot entry P27037, amino acid residues 20 to 134) with a C-terminal APP-tag (EFRHDS) was expressed transiently in HEK293-6E cells in a 10L Biowave reactor using a 1:1 mix of V3 and DM133 culture media. Concentrated cell culture supernatant (1.3l) was applied to a 25 ml anti-APP Sepharose 4B column at 1 ml/min overnight. After baseline washing with PBS pH 7.3, bound material was eluted with 0.1M Glycine, pH 2.7, adjusted to pH 7.6 with 2M NaOH and sterile filtered. The eluate was concentrated to 5ml in an Amicon stirred cell (MWCO 3000) and loaded on a HiLoad XK16/600 Superdex 200 Prep Grade column run in PBS pH 7.3. Fractions were analyzed by SDS-PAGE under non-reducing conditions and those containing monomeric protein were pooled, yielding 2.4mg of ActRIIA-LBD.

Expression and Purification of the ActRIIB-LBD. The ActRIIB-LBD (Uniprot entry Q13705, amino acid residues 24 to 117) was cloned as a thioredoxin-His6-fusion protein, with a PreScission cleavage site inserted after the His6-tag and expressed intra-cellularly in *E. coli* Shuffle. Cells were grown at 37°C in LB medium with carbenicillin (100mg/l) up to an OD_{600nm} of 1.6, then cooled down to 16°C, induced overnight with IPTG (0.1mM), and cultivated at 16°C up to an OD_{600nm} of 2.7.

Cell pellets (5.2g) were suspended in 100ml of lysis buffer (50mM TRIS pH 8.0, 0.5M NaCl, 10% glycerol, with 1 tablet of EDTA-free complete protease inhibitor cocktail (Roche) per 50ml buffer, lysed with a French press and centrifuged with a SS34 rotor at 18,000rpm. The supernatant was then loaded onto a 5ml Crude FF metal chelation column equilibrated with

50mM TRIS pH 8.0, 0.5M NaCl, 10% glycerol. After a washing step with 25mM imidazole, the thioredoxin fusion protein (34mg) was eluted by an imidazole gradient (25 to 500mM imidazole).

Purification and crystallization of the ActRIIB-LBD Fv complex. The Bimagrumab V_H (residues 1 to 115 with a carboxy-terminal His_6-tag) and V_L (residues 1 to 111 with a carboxy-terminal Strep-tag) regions were cloned and expressed on a single polycistronic, periplasmic expression vector in *E. coli* W3110. Cells were cultivated at 25°C in SB medium with tetracycline (12.5µg/ml) and expression was induced with 0.5mM IPTG. Cell pellets were suspended in 150ml lysis buffer (20mM NaH_2PO_4, 10mM imidazole, 500mM NaCl, pH 7.4, with benzonase and 1 tablet of EDTA-free cOmplete protease inhibitor cocktail (Roche) per 50ml buffer), and disrupted by sonication on ice. After centrifugation at 4°C, the supernatant was sterile filtered and loaded on a 2ml HisTrap column (GE-Healthcare) equilibrated with lysis buffer. After a washing step with 20mM imidazole, the Fv was eluted with a 20 to 500mM imidazole gradient. Fractions were analyzed by SDS-PAGE (NuPage, Invitrogen), pooled, concentrated by ultrafiltration and loaded onto a Superdex75 column (HiLoad 16/60, GE-Healthcare). After isocratic elution in 10mM Tris-HCl, pH 7.5, 25mM NaCl, fractions were analyzed by SDS-PAGE, pooled and concentrated by ultrafiltration.

A 1.4-fold molar excess of the thioredoxin-His_6-PreSc-ActRIIB(24-117) fusion protein was mixed with the Bimagrumab Fv and cleavage was performed on the protein complex by adding 4% (w/w) PreScission protease and dialyzing the reaction mixture overnight against 50mM TRIS pH 8.0, 50mM NaCl. The reaction mixture was then loaded on a monoQ ion exchange chromatography column equilibrated in 50mM TRIS pH 8.0, 50mM NaCl. The Fv complex was in the flow-through, while excess ActRIIB-LBD was retained by the ion exchange column. Pooled fractions of the Fv complex were further purified by size exclusion chromatography

(SPX-75). The Fv complex was then concentrated to 6-10mg/ml and submitted to crystallization screening as described above. Cubic crystals diffracting to 3.35Å were first obtained from 1.4M ammonium sulfate, 0.1M sodium acetate pH 4.6. For data collection, these crystals were cryo-protected with 1.8M ammonium sulfate, 0.1M sodium citrate pH 4.6, 20% glycerol and flash frozen. A second, orthorhombic crystal form diffracting to 2.0Å grew after 2 months from 0.1M phosphate-citrate buffer pH 5.4, 40% PEG 300. One crystal was directly harvested and frozen in liquid nitrogen for data collection.

Purification and crystallization of the ActRIIA-LBD Fv complex. The Bimagrumab Fv and the ActRIIA-LBD were mixed at a 1:1 molar ratio and the complex was purified by size exclusion chromatography (SPX-75) in 10mM Tris-HCl pH 7.4, 100mM sodium chloride, and concentrated by ultrafiltration to 12.6mg/ml. Crystallization screening was performed as described before. Monoclinic crystals of the Fv complex with the ActRIIA-LBD grew within 5 days from 0.1M sodium citrate tribasic, 25% w/v PEG 3350. Before flash-freezing in liquid nitrogen, one crystal was transferred into reservoir solution supplemented with 20% glycerol (v/v) and incubated for 10s.

Crystallographic data collection, structure determination and refinement. All diffraction data were collected at the Swiss Light Source, beamlines PX-II and PX-III, with a MAR CCD 225mm (Fab and Fv complex with ActRIIB-LBD) or a Pilatus detector (ActRIIA-LBD complex). Diffraction images were processed with HKL2000 (1) or XDS (2). Data collection statistics are summarized in Supplementary table 1. The structure of the free Fab was solved by molecular replacement with Phaser (3), using PDB entry 2JB5. The variable and first constant domains were used as independent search models. The model was rebuilt in Coot (4) and initially refined with CNX 2002 (5). Final refinement runs were performed with AutoBuster(6). The structure of

the Fv complex with the ActRIIB-LBD was first determined at 3.35Å resolution from the cubic crystal form by molecular replacement with Phaser, using as search models the V_H/V_L domain of the previously-determined Bimagrumab Fab structure and the ActRIIB-LBD from PDB entry 2H64 (2). Iterative model building and refinement were performed with Coot and CNX 2002. Then, this low resolution model was used to solve the structure of the orthorhombic crystal form with Phaser. Model building and refinement against the 2.0Å resolution data set was carried out as described above for the free Bimagrumab Fab. The structure of the Fv complex with the ActRIIA was similarly determined with Phaser using the ActRIIB-LBD complex as search model, and refined with Coot and Autobuster. Final refinement and crystallographic model statistics are provided in Supplementary table 1. The antigen-antibody interface was analyzed with the CCP4 programs (7) AREAIMOL and NCONT. Figures were prepared in PyMol (8).

1. Otwinowski Z, Minor W (1997) Processing of X-ray diffraction data collected in oscillation mode. *Methods Enzym* 276:307–326.
2. Kabsch W (1993) Automatic processing of rotation diffraction data from crystals of initially unknown symmetry and cell constants. *J Appl Crystallogr* 26:795-800.
3. McCoy AJ, *et al*. (2007) Phaser crystallographic software. *J Appl Crystallogr* 40:658-674.
4. Emsley P, *et al*. (2010) Features and development of Coot. *Acta Crystallogr D Biol Crystallogr* 66:486-501.
5. Brünger AT, *et al*. (1998) Crystallography & NMR system: A new software suite for macromolecular structure determination. *Acta Crystallogr D Biol Crystallogr* 54:905-921.
6. Bricogne G, *et al*. BUSTER version 2.11.2. Cambridge, United Kingdom: Global Phasing Ltd (2011).
7. Winn MD, *et al*. (2011) Overview of the CCP4 suite and current developments. *Acta Crystallogr Sect D Biol Crystallogr* 67:235-242.
8. DeLano WL. Pymol Molecular Graphics System (DeLano Scientific, San Carlos, California, 2002).

SI Figure S1

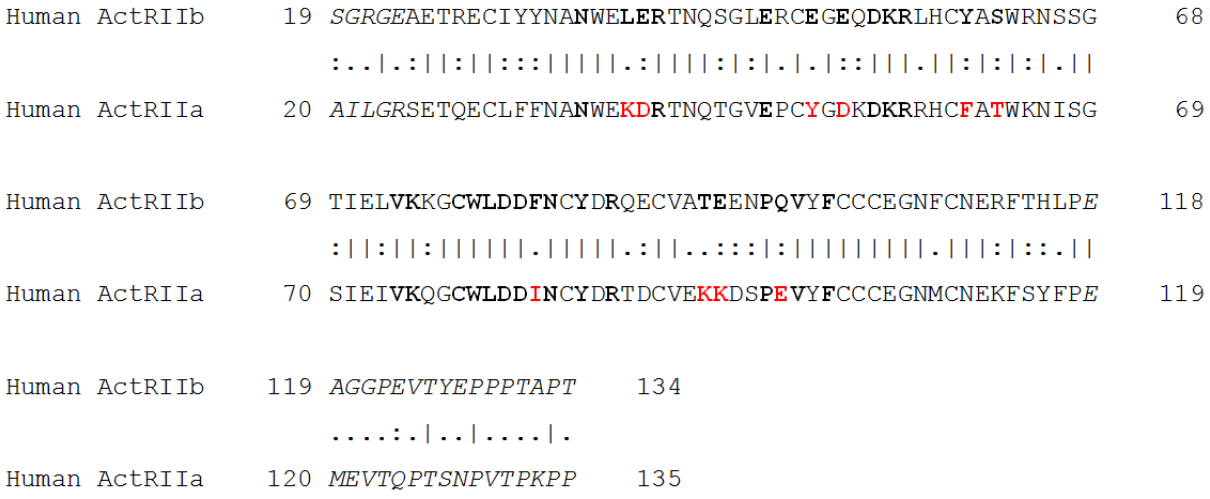

Sequence alignment of the human ActRIIA- and ActRII-LBD. Amino-acid sequence alignment of the human ActRIIB and ActRIIA ligand binding domains (generated with the Needle program using a gap open penalty of 10 and a gap extend penalty of 1.0). Residues in bold font are located at the Bimagrumab binding interface in the ActRIIB complex. ActRIIA residues highlighted in bold red are not conserved. Italicized residues were not included in the recombinant ActRIIB LBD used in this work.

SI Figure S2

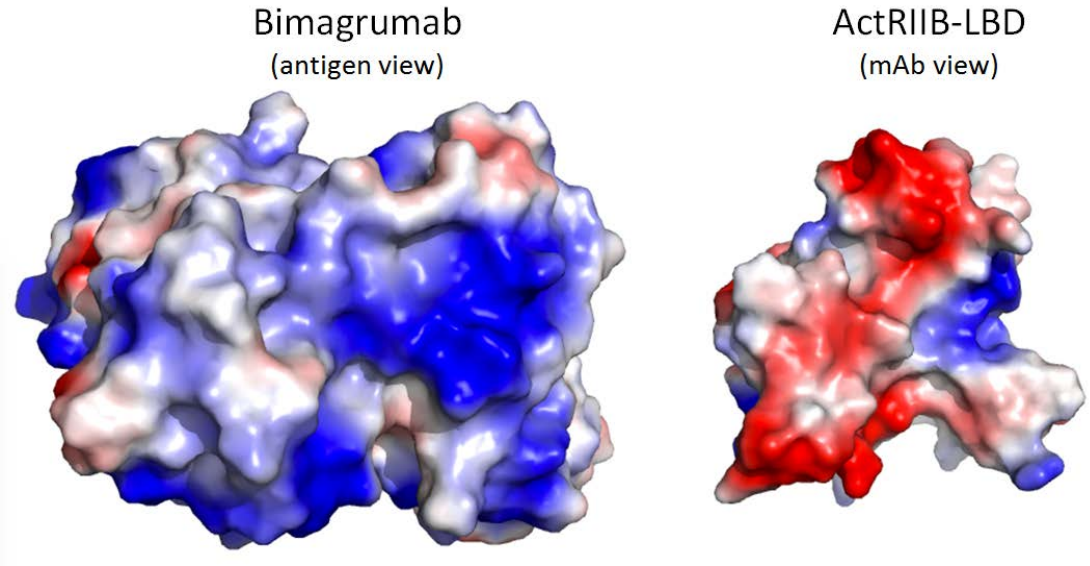

Electrostatic complementarity of the antibody-antigen interface. “Open book view” of the antibody-antigen interface, showing electrostatic potential surfaces. Note the electrostatic complementarity of the mainly basic (blue patches) antigen-combining site of Bimagrumab with the mainly acidic (red patches) ActRII-LBD epitope (ActRIIB-LBD shown here as an example).

SI Figure S3

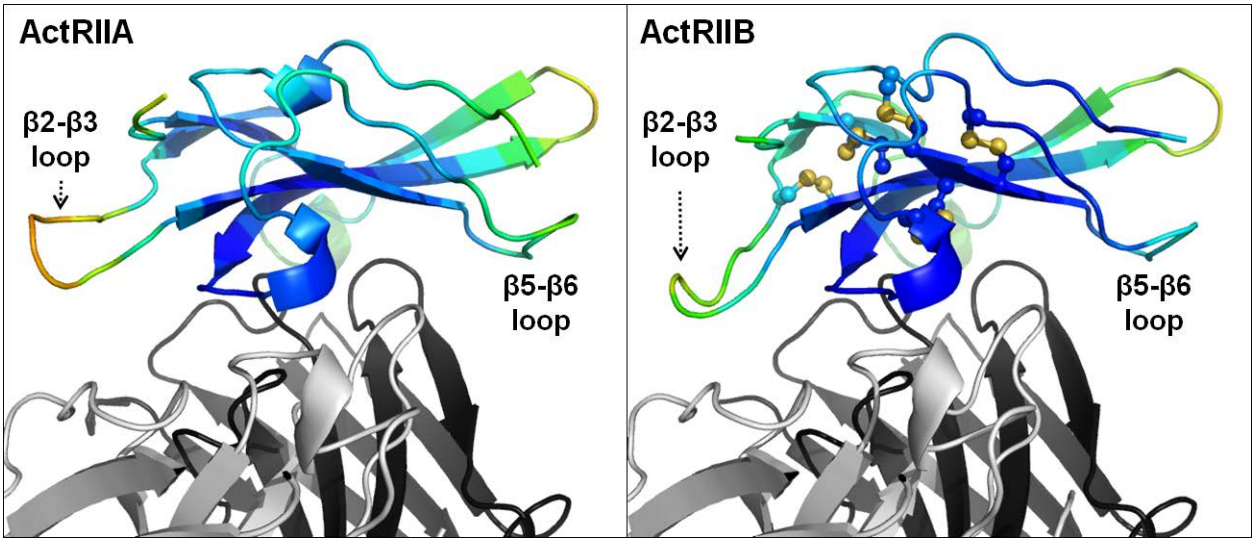

Close-up view of the Bimagrumab-bound ActRII-LBD shown in ribbon representation and color-coded according to temperature factors. Left panel: ActRIIA-LBD complex. Right panel: ActRIIB-LBD complex. Note that the β2-β3 and the β5-β6 loops have higher temperature factors in the ActRIIA-LBD complex, and that the β2-β3 loop in ActRIIA is located farther from the antibody.

SI Figure S4

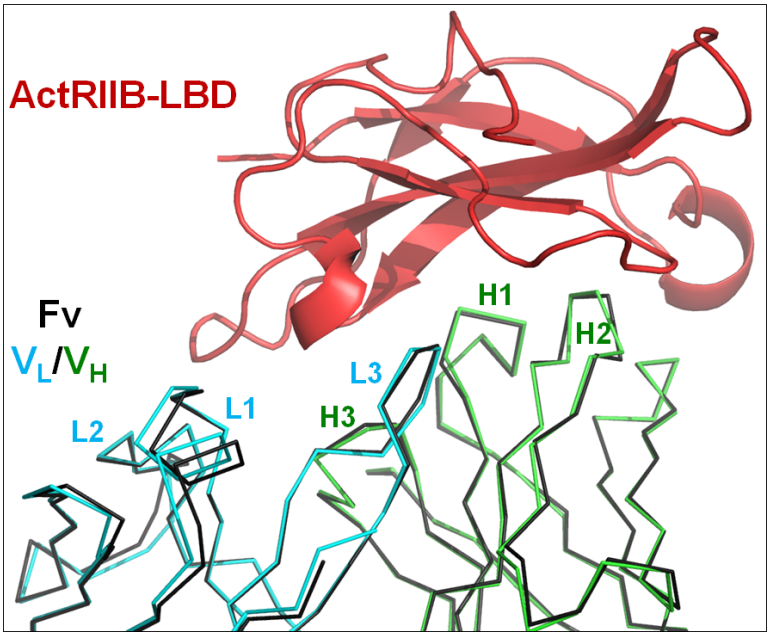

Structural overlay of the free- (black Cα trace) and ActRIIB-bound (cyan and green Cα traces) states of the Bimagrumab variable domains. The protein antigen is shown as a red cartoon. Light- and heavy-chain CDR loops are labelled L1 to L3 and H1 to H3, respectively. Note the small shift of the L-CDR1 loop upon antigen binding.

SI Figure S5

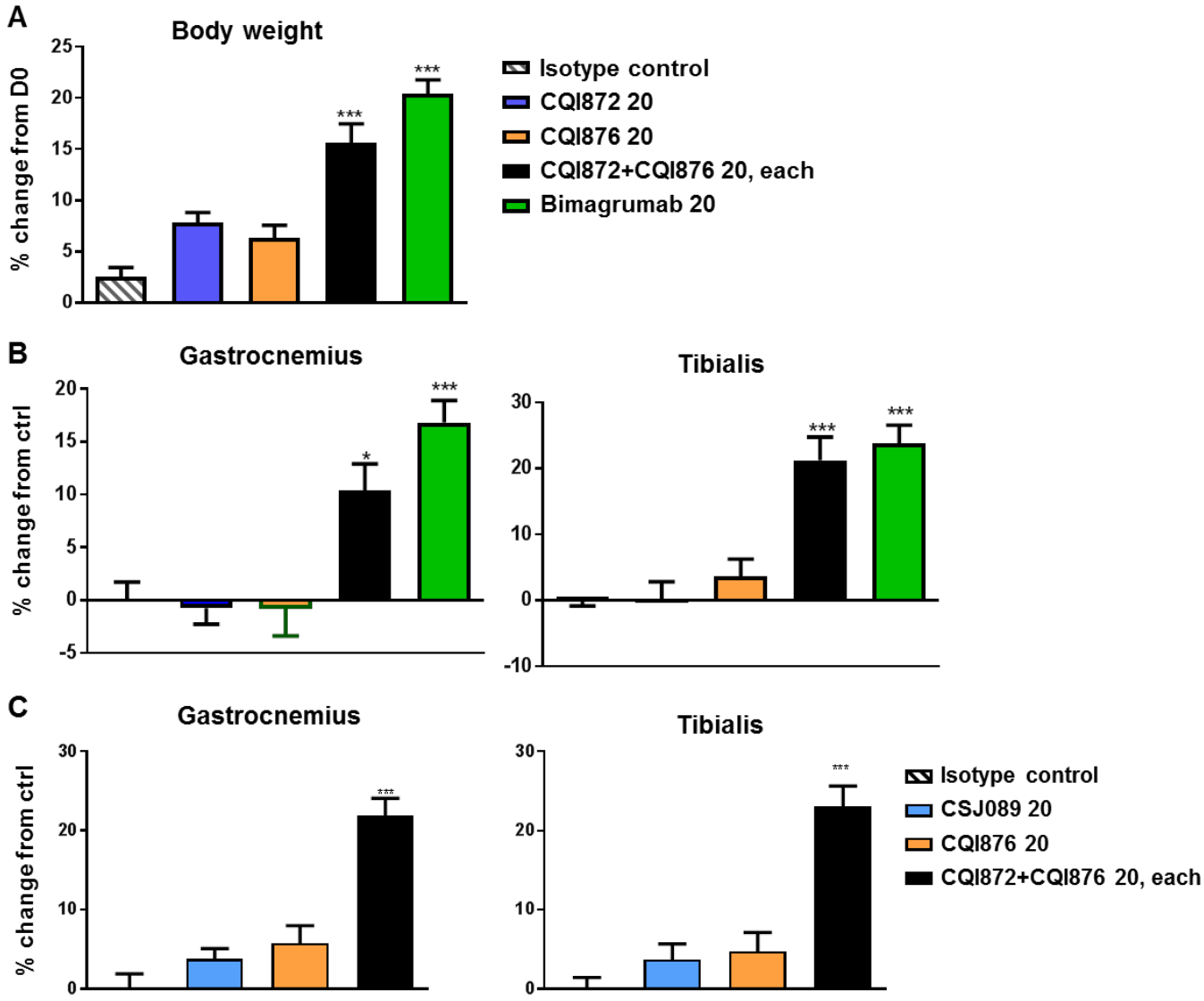

Hypertrophy response as measured via (*A*) body weight, (*B*) muscle weight changes after 2 weeks of weekly s.c. treatment of SCID mice with 20mg/kg/week of isotype control antibody (stripes) or an anti-ActRIIA Ab (CQI872, blue, KD:28pM), an anti-ActRIIB Ab (CQI876, orange, KD:64pM) , a combination of anti ActRIIA and anti-ActRIIB Abs (black), or Bimagrumab (green). (*C*) Muscle hypertrophy response after 4 weeks of weekly i.v. treatment of Wistar rats with anti-ActRIIA Ab (CSJ089, blue, KD:488pM), an anti-ActRIIB Ab (CQI876, orange, KD:64pM), a combination of anti ActRIIA and anti-ActRIIB Abs (black). . Data are presented as mean±SEM analyzed using 1-way ANOVA; differences after Bonferroni test were considered statistically signicant, *P<0.05; ***P<0.01

SI Table S1 Diffraction data and refinement statistics.

	Free Fab	**ActRIIA-LBD Fv complex**	**ActRIIB-LBD Fv complex** Cubic crystal form	**ActRIIB-LBD Fv complex** Orthorhombic crystal form
Data collection				
Beamline	SLS/PXII	SLS/PXII	SLS/PXII	SLS/PXIII
Detector	MAR CCD 225mm	Pilatus	MAR CCD 225mm	MAR CCD 225mm
Processing software	HKL2000	XDS/XSCALE	HKL2000	XDS/XSCALE
Space group	$P2_12_12_1$	$P2_1$	P23	I222
a, b, c (Å)	44.0, 78.0, 131.3	44.3, 108.2,100.7	187.8,187.8,187.8	62.1, 114.2,117.9
α, β, γ (°)	90.0, 90.0, 90.0	90.0, 98.3, 90.0	90.0, 90.0, 90.0	90.0, 90.0, 90.0
Resolution (Å)	1.78 (1.84-1.78)	2.35 (2.41-2.35)	3.35 (3.47-3.35)	2.00 (2.05-2.00)
R_{sym} or R_{merge}	0.094 (0.470)	0.089 (0.60)	0.093 (0.482)	0.070 (0.62)
I / σ(I)	6.0 (2.8)	11.86 (2.2)	8.2 (2.8)	14.2 (2.2)
Completeness (%)	100.0 (100.0)	97.9 (97.3)	90.6 (93.9)	99.8 (100.0)
Redundancy	6.2 (6.0)	3.5 (3.5)	3.3 (3.2)	14.2 (13.8)
Refinement				
Resolution (Å)	41.74-1.78	47.55-2.35	50.00-3.35	17.05-2.00
No. reflections	19,638	38,338	30,060	28,614
R_{work} / R_{free}	0.179 / 0.207	0.168 / 0.208	0.216 / 0.229	0.178/ 0.198
No. atoms				
Protein	3,134	4,816	4,924	2,475
Buffer component	0	0	0	13 (PEG)
Waters	483	361	0	174
B-factors (Å^2)				
Ab light-chain	24.0 / -	33.6 / 35.1	66.1 / 65.7	36.3
Ab heavy-chain	19.9 / -	33.4 / 38.7	72.0 / 72.3	35.8
ActRII-LBD	- / -	48.4 / 48.0	79.2 / 79.0	59.5
Waters	40.1	46.2	-	46.1
R.m.s. deviations				
Bond lengths (Å) / angles (°)	0.010 / 1.09	0.010 / 1.10	0.008 / 0.94	0.010 / 1.03
Ramachandran statistics				
Favored (%)	95.95	96.65	91.35	96.15
Allowed (%)	3.81	3.03	6.25	3.21
Outliers (%)	0.24	0.32	2.40	0.64

Numbers in brackets correspond to the high resolution shell.

SI Table S2 General descriptors of the antigen-antibody interface.

	ActRIIA-LBD complex with Bimagrumab Fv (chain A)	**ActRIIB-LBD complex with Bimagrumab Fv** (Orthorhombic crystal form)
ActRII-LBD residues with reduced solvent-accessible surface	N36, K39, D40, E48, D55, R58, F61, T63, V74, K75, C78, W79, L80, D81, D82, I83, N84, Y86, V100, F102	N35, L38, E39, R40, E47, E50, E52, D54, K55, R56, Y60, S62, V73, K74, C77, W78, L79, D80, D81, F82, N83, Y85, R87, T93, E94, P97, Q98, V99, F101
Total	**20**	**29**
Bimagrumab-CDR residues with reduced solvent-accessible surface		
L-CDR1	Y32, N33, Y34	Y32, N33, Y34
L-CDR2	Y51, K55, R56, S58	Y51, K55, R56, P57, S58
L-CDR3	F93, G95, G96, S97, Y98	F93, G95, G96, S97, Y98
Total light-chain	12	13
H-CDR1	Y27, T28, T30, S31, S32, Y33	G26, Y27, T28, T30, S31, S32, Y33
H-CDR2	N52, P53, V54, S55, S57	N52, P53, V54, S55, S57, T58
H-CDR3	R98, G99, G100, W101, D103	R98, G99, G100, W101, D103, Y104
Total heavy-chain	16	19
Total antibody	**28**	**32**
Buried solvent accessible surface		
ActRII-LBD ($Å^2$)	-798.1	-1052.9
Bimagrumab		
- Light-chain	-156.7	-266.4
- Heavy-chain ($Å^2$)	-591.9	-726.4
Total Bimagrumab ($Å^2$)	-748.5	-992.8
Total combined buried surface ($Å^2$)	-1546.6	-2046.7
Surface complementarity statistic	0.796	0.771

SI Table S3

	HEK293T/17 cells MFI
Isotype control Ab	12 ± 0.5
CSJ089, anti-ActRIIA Ab	100 ± 10.6
CQI876, anti-ActRIIB Ab	81 ± 8.3
CSJ089 + CQI876	129 ± 14.9
Bimagrumab	190 ± 39.7

Mean fluorescence intensity (MFI) of anti-ActRIIA Ab, anti-ActRIIB Ab, anti-ActRIIA and ActRIIB Abs combination, Bimagrumab or isotype control Ab to HEK293T/17 cells, average±SEM of 3 independent experiments.

SI Table S4

		RGA			
		Myostatin		Activin A	
Antibodies	**Specificity**	IC50 [nM]	max. inhib. [%]	IC50 [nM]	max. inhib. [%]
CSJ089	ActRIIA	0.32	47	0.44	35
CQI876	ActRIIB	0.37	50	1.15	30
CSJ089 + CQI876	combo	0.31	93	1.14	96
Bimagrumab	pan	0.04	96	0.58	97
CDD861	pan	0.06	94	0.23	96

Efficacy / potency of antibodies or combination thereof at blocking Myostatin or activin A induced Smad2/3 response. Single specificity Abs, or combination thereof, or Bimagrumab were tested for their ability to inhibit myostatin (10ng/ml) or activin A (10ng/ml) induced Smad2/3 reponse in a CAGA-luciferase reporter gene assay using stably transfected into HEK293 T/17 cells. Results are average of 3 to 6 independent experiments.

SI Table S5

	Gastroc	Quadriceps	Tibialis	EDL	Soleus
CSJ089 Ab 6mg/kg	11.52±1.60*	11.57±2.27*	2.27±2.67	6.48±4.02	10.07±4.01
CSJ089 20mg/kg	9.23±1.79*	8.70±1.73	5.37±2.49	-2.84±1.35	16.21±4.77
CQI876 6mg/kg	8.76±2.16*	11.11±2.42*	6.73±2.59	11.99±2.75	11.38±1.53
CQI876 20mg/kg	6.47±3.16	7.30±2.26	4.67±1.82	11.98±5.18	1.01±3.77
CSJ089 + CQI876 6mg/kg, each	18.24±3.27*	26.94±1.95*	25.41±2.48*	17.73±3.17	20.25±6.05*
CSJ089 + CQI876 20mg/kg, each	27.7±2.19*,#	32.32±1.99*	29.56±1.75*	24.84±6.52	40.06±7.10*,#
Bimagrumab 6mg/kg	20.91±3.12*	22.40±1.96*	24.79±1.79*	23.55±4.60	20.79±5.25*
Bimagrumab 20mg/kg	26.66±1.41*	32.72±1.85*,#	31.75±2.18*,#	16.36±9.78	36.34±2.98*,#
Sham	-4.10±1.77	-5.91±1.20	-8.96±2.54	-10.74±2.81	-5.99±4.26
Control	0.0±1.40	0.0±1.61	0.0±1.63	0.0±7.09	0.0±8.25